AFOSR-TR. 81-0543

LEVEL II

department of chemical engineering and fuel technology

DTIC
SELECTE
JUL 7 1981
D

C

81 7 06 015

JUL 7 1981

DROPLET TRAJECTORIES IN THREE-DIMENSIONAL

GAS TURBINE FLOW FIELDS.

W.H. Ayers, F. Boysan and J. Swithenbank

Department of Chemical Engineering and
Fuel Technology, University of Sheffield
Sheffield. S1 3JD

REPORT DOCUMENTATION PAGE	READ INSTRUCTIONS BEFORE COMPLETING FORM

1. Report Number	2. Govt Accession No.	3. Recipient's Catalog Number
AFOSR-TR-81-0543	AD-A101 883	

4. Title (and Subtitle)	5. Type of Report & Period Covered
DROPLET TRAJECTORIES IN THREE-DIMENSIONAL GAS TURBINE FLOW FIELDS	*Interim*
	6. Performing Org. Report Number

7. Author(s) W.H Ayers, F. Boysan, J. Swithenbank.	8. Contract or Grant Number AFOSR 80-0174 ✓

9. Performing Organization Name and Address University of Sheffield, Mappin Street, Sheffield S1 3JD, U.K.	10. Program Element, Project, Task Area & Work Unit Numbers 61102F 2308/A2

11. Controlling Office Name and Address Air Force Office of Scientific Research/NA, Building 410, Bolling Air Force Base, DC 20332	12. Report Date September 1980
	13. Number of Pages 18

14 Monitoring Agency Name and Address	15. *Unclassified*

16. & 17. Distribution Statement

Approved for public release; distribution unlimited.

18. Supplementary Notes

19. Key Words

Combustion	2 phase flow
Modelling	Gas turbine combustor
Spray	Combustor design

20. Abstract ,Much work is currently being carried out in the field of mathematical modelling of the physical and chemical processes taking place within combustion equipment to enable better combustion chamber design. One aspect of this is the numerical prediction of burning droplet trajectories in a gas flow field and in this paper a general three-dimensional particle/droplet trajectory algorithm is presented and applied to fuel sprays in gas turbine combustors. Droplet evaporation and initial heating up effects are included and trajectories are calculated within a three-dimensional computer predicted gas flow field. By injecting many droplets with initial conditions representing a particular fuel nozzle a complete fuel spray can be constructed, and this is presented graphically. The results show that in some cases the three-dimensional nature of the gas flow and the behaviour of large droplets may be expected to have a significant effect on combustor performance.

FORM 1473

DROPLET TRAJECTORIES IN THREE-DIMENSIONAL GAS TURBINE FLOW FIELDS

W.H. Ayers, F. Boysan and J. Swithenbank
Department of Chemical Engineering and Fuel Technology
University of Sheffield.

Abstract

Much work is currently being carried out in the field of mathematical modelling of the physical and chemical processes taking place within combustion equipment to enable better combustion chamber design. One aspect of this is the numerical prediction of burning droplet trajectories in a gas flow field and in this paper a general three-dimensional particle/ droplet trajectory algorithm is presented and applied to fuel sprays in gas turbine combustors. Droplet evaporation and initial heating up effects are included and trajectories are calculated within a three-dimensional computer predicted gas flow field. By injecting many droplets with initial conditions representing a particular fuel nozzle a complete fuel spray can be constructed, and this is presented graphically. The results show that in some cases the three-dimensional nature of the gas flow and the behaviour of large droplets may be expected to have a significant effect on combustor performance.

Nomenclature

C_b	Evaporation constant
C_D	Drag coefficient
C_p	Specific heat capacity at constant pressure
D_p	Droplet or particle diameter
$\bar{D}$	Rosin-Rammler mean diameter
I,J,K	Finite difference grid subscripts in axial, radial and tangential directions.
L	Latent heat of evaporation
m	Mass
$\dot{m}$	Mass flowrate
n	Rosin-Rammler spread parameter
Nu	Nusselt number
Pr	Prandtl number
Re	Reynolds number
t	Time
T	Temperature
u	Velocity vector
u, v, w	velocity components in axial, radial and tangential directions
$\dot{u}, \dot{v}, \dot{w}$	time derivatives of u, v and w
x, y, θ	distance in axial, radial and angular directions.
$\dot{x}, \dot{y}, \dot{\theta}$	time derivatives of x, y and θ
ρ	Density
μ	Viscosity
λ	Thermal conductivity

Subscripts:

o	Initial
∞	Gas flow
g	Gas
ℓ	Liquid
p	particle or droplet

Introduction

The availability of large general purpose digital computers has enabled numerical techniques to be applied to many complex engineering problems. In the field of Combustion Research mathematical modelling can be used to predict the behaviour of all kinds of combustion processes and such numerical procedures are forming the basis of a more systematic approach to combustion equipment design. The aim of current work on Gas Turbine Combustor modelling is to provide a design tool to assist in what is at present a largely empirical process of combustor design. This is a field of increasing importance as a result of present interest in fuel economy and pollution control.

Algorithms have been produced capable of modelling the chemical and physical processes occuring in a gas turbine combustor can and these are reviewed by Swithenbank et al (Ref. 1). These models do not, however, include the details of two-phase flow and droplet combustion arising from the injection of a liquid fuel spray. The fate of burning droplets in a gas flow has so far only been considered in two dimensions (Ref. 2). Other related work includes that of Law (Ref. 3) who analyses the motion of an evaporating droplet in a constant cross flow, and Chiu et al (Ref. 4) who present a model for the collective behaviour of burning droplets in liquid fuel sprays. Mellor (Ref. 5) has represented the dominant processes of spray combustion by means of time scales for evaporation, mixing and chemical reaction. Dring and Suo (Ref. 6) have obtained particle trajectories in swirling flows and subsequently in turbine cascades (Ref. 7).

At present the detailed behaviour of fuel droplets during spray combustion is largely unknown and experimental data are difficult, if not impossible to obtain. These phenomena affect all aspects of the combustion process and a full understanding of spray combustion is required before rigorous design techniques can be employed.

In this study a general algorithm is produced to calculate the trajectories of particles or evaporating/burning droplets in a three-dimensional gas flow field represented by a finite difference grid, and this is applied to fuel sprays in a gas turbine combustor. The results predict in detail the behaviour of individual burning droplets and the distribution of vaporised (unburnt) fuel in the combustor can.

Theory

Because of the cylindrical nature of combustion chambers and the gas flows involved, a cylindrical polar coordinate system is used to describe the location of the particle or droplet. The equations of motion of a particle, neglecting all forces except drag, in component form are:

$$\dot{u}_p = -\frac{18\,\mu_g}{\rho_\ell\,D_p^2}\;\frac{C_D\,R_e}{24}\;(U_p - U_\infty) \tag{1}$$

$$\dot{v}_p = \frac{w_p^2}{y_p} - \frac{18\mu_g}{\rho_\ell\,D_p^2}\;\frac{C_D\,R_e}{24}\;(v_p - v_\infty) \tag{2}$$

$$\dot{w}_p = \frac{-v_p w_p}{y_p} - \frac{18\mu_g}{\rho_\ell\,D_p^2}\;\frac{C_D\,R_e}{24}\;(w_p - w_\infty) \tag{3}$$

where u_p, v_p and w_p are the absolute particle velocities in the axial, radial and tangential directions respectively, and u_∞, v_∞ and w_∞ are the corresponding gas velocities.

For the cylindrical polar coordinate system, the equations of trajectory are:

$$\dot{x}_p = u_p \tag{4}$$

$$\dot{y}_p = v_p \tag{5}$$

$$\dot{\theta}p = \frac{w_p}{y_p} \tag{6}$$

where x_p, y_p and θ_p are the distances of the particle from the origin in the axial, radial and angular directions.

In the above equations the relative Reynolds number, R_e is defined as:

$$R_e = \frac{D_p\,\rho_g}{\mu_g}\;\left|\;\vec{u}_p - \vec{u}_\infty\;\right| \tag{7}$$

where $\vec{u}_p$ and $\vec{u}_\infty$ are the velocity vectors of the particle and gas stream respectively.

The drag coefficient, C_D, is given by the following equations (Ref. 8):

- 4 -

$$C_D = 27 \, R_e^{-0.84} \qquad 0 < R_e < 80 \qquad\qquad (8)$$

$$C_D = 0.271 \, R_e^{0.217} \qquad 80 < R_e < 10^4 \qquad\qquad (9)$$

$$C_D = 2 \qquad\qquad 10^4 < R_e \qquad\qquad (10)$$

Equations (1) to (10) describe the trajectory of a particle in a gas stream. For an evaporating droplet, D_p is not constant, and the rate of change of droplet diameter with time is required. For forced convection this is given by:

$$\frac{dD_p}{dt} = -\frac{C_b}{2D_p} \, (1 + 0.23 \, R_e^{\frac{1}{2}}) \qquad\qquad (11)$$

where C_b is the evaporation constant. This is dependant on the properties of the fuel as well as the surrounding gases, and a widely used expression for C_b derived from the quasi-steady analysis of droplet combustion is that given by Wise and Agoston (Ref. 9)

$$C_b = \frac{8\lambda_g}{\rho_\ell \, C_{pg}} \cdot \ln\left[1 + \frac{C_{pg}}{L} \, (T_\infty - T_\ell) \right] \qquad\qquad (12)$$

To allow for droplets "heating up" after entry into the hot gas stream it has been assumed that droplets do not begin to evaporate until they reach their boiling point. The rate of change of temperature with time is given by:

$$\frac{dT_p}{dt} = \frac{6 \, Nu \, \lambda_g}{\rho_\ell \, D_p^2 \, C_{p\ell}} \cdot (T_\infty - T_p) \qquad\qquad (13)$$

where T_p is the droplet temperature.

If it is assumed that the Reynolds number varies slowly with respect to time, it is possible to integrate equations (11) and (13) for small increments of time so that equation (11) becomes:

$$D_p^2 = D_{po}^2 - C_b(1 + 0.23 \, R_e^{\frac{1}{2}})(t - t_o) \qquad\qquad (14)$$

giving the droplet diameter D_p at time t, where D_{po} is the droplet diameter at time t_o. Equation (13) is integrated to give:

$$T_p = T_\infty - (T_\infty - T_{po}) \exp\left[\frac{-6Nu\lambda_g}{\rho_\ell D_p^2 C_{p\ell}} \cdot (t-t_o)\right] \qquad (15)$$

where T_{po} is the drop temperature at time t_o.

Equation (13) is suppressed until the droplet temperature, reaches the boiling point of the liquid, after which T_p remains constant. The Nusselt number, Nu is given in Refs. 10 and 11 as:

$$Nu = 2 + 0.6 \ R_e^{\frac{1}{2}} \ Pr^{1/3} \qquad (16)$$

where the Prandtl number, Pr is given by:

$$Pr = \frac{C_{pg} \ \mu_g}{\lambda_g} \qquad (17)$$

Equations (1) to (17) above describe the motion of an individual evaporating droplet in three dimensions in a gas stream. Numerical integration can now be used to calculate the droplet trajectory in the given gas flow field.

Application

For the purposes of this investigation a computer predicted flow field in a gas turbine combustor was used. This has been calculated for a Lycoming combustor using a numerical prediction algorithm to model the physical and chemical processes taking place (Ref. 12).

The geometry of the Lycoming combustor can, which was designed as research combustor, is shown in Fig.1. Air enters via a swirler which produces a finite swirl velocity. The fuel spray is introduced at a point near the centre line in front of a baffle and is of hollow cone type. Primary, secondary and dilution air streams are introduced by three sets of injection holes, each consisting of six equally spaced circular orifices around the periphery of the combustor can. This is responsible for the three-dimensional nature of the problem, and the cyclic nature of the flow enables the combustor can to be represented by a single 60° sector, which is divided into a 27 x 18 x 7 element grid in the x, y and θ directions respectively. The grid is shown diagramatically in Fig. 2.

Each grid node is encompassed by a computational cell which is used to store temperature and density data. Gas velocity data, however, is defined for staggered control volumes as shown in Fig. 3. For droplet trajectory calculations these data are redefined to refer to the same nominal control volumes as used to store temperature and density data,

- 6 -

by averaging adjacent velocity values. This considerably simplifies the subsequent trajectory calculations.

The two-dimensional model of Reference 2 assumes that the gas flow field is essentially two-dimensional in the region of the fuel spray. To investigate the validity of this assumption, a statistical analysis of axial velocity data was made. For each value of I and each of three J values the set of data for all K values was averaged and sample standard deviation calculated. The result of this analysis is given in Fig. 4 and shows that the flow is essentially two-dimensional until a short distance upstream of the first (primary) set of air injection holes. Beyond this point the flow becomes predominantly three-dimensional, particularly in the vicinity of the air injection holes. It can also be seen that flow is axisymetric near to the axis (J=3).

A vector plot of the velocity field is given in Fig. 5. It can be clearly seen that there is a recirculation zone in front of the baffle, and that the flow in the region of the air injection holes is dominated by the inward flow of air. The flow cross-section at the point of primary air inlet shows how the three-dimensional nature of the flow field is brought about by the air injection.

Once the u-, v-, w-velocity, temperature and density data is stored as a 27 x 18 x 7 element array, the fundamental equations of motion and trajectory (equations 1 to 6) can be solved numerically by assuming that the gas velocity, temperature and density remain constant throughout each computational cell. These six simultaneous differential equations are solved by using the fourth order Runge-Kutta method for a short time step, the length of which is adjusted automatically to give approximately the same number of time steps while the droplet is in each cell.

After solving the equations for one time step the new drag coefficient and Reynolds number are calculated and one of equations (14) or (15) is used depending on whether the droplet has reached its boiling point. Computation for the next time increment then proceeds unless the droplet has passed out of the computational cell. In this case the new cell that the droplet occupies is determined and the iteration is resumed. At this stage a check is also made for droplets passing into an adjacent sector (in which case they are made to re-enter the original sector at the symetrically corresponding position), and for other contingencies which may terminate the iteration procedure, e.g. droplets vanishing by

evaporation, colliding with the walls of the combustor can, etc.

The amount of fuel evaporated per unit time in each cell is calculated for each droplet as it leaves the cell as:

$$\dot{m}_{evap} = \frac{D_{out}^3 - D_{in}^3}{D_{initial}^3} \cdot \dot{m}_{fuel} \tag{18}$$

where D_{in} is the droplet diameter on entering the cell, D_{out} the exit diameter and $D_{initial}$ the droplet diameter at the start of its trajectory. The total mass flowrate of fuel represented by the droplet is $\dot{m}_{fuel}$.

If the droplet hits a wall the remaining fuel contained in the droplet is deposited into the cell adjacent to the wall, representing droplets adhering to the wall of the combustion chamber. It would be possible here to extend the model to include droplets rebounding off the wall, shattering etc.

To extend the model to predict the behaviour of a whole spray, a statistical size distribution is used to represent the spray as a number of size ranges, each represented in turn by a single droplet diameter, the mean of the size range. Inherent in this approach is the assumption that an individual droplet trajectory is unaffected by the presence of other droplets in the droplet cloud. This is valid if the rate of reaction (i.e. combustion) of fuel vapour is sufficiently high to prevent a significant partial pressure of unburnt fuel vapour existing between droplets.

It is assumed that after sheet break-up, the fuel spray leaving the atomiser obeys a Rosin-Rammler size distribution. In this model the mass fraction of fuel having a droplet diameter greater than D is given as:

$$m_D = exp\left[-\left(\frac{D}{\bar{D}}\right)^n \right] \tag{19}$$

where $\bar{D}$ is the Rosin-Rammler mean diameter and n is the spread parameter. For this study a value 66 microns was chosen for $\bar{D}$ and the spread parameter is taken as 2.5. These values were derived from experimental data for a typical nozzle obtained by Pan (Ref. 13). The mass fraction of fuel in a given size range is found by subtraction :

$$m_{range} = \left| exp\left[-\left(\frac{D_1}{\bar{D}}\right)^n \right] - exp\left[-\left(\frac{D_2}{\bar{D}}\right)^n \right] \right| \tag{20}$$

- 8 -

where the size range lies between D_1 and D_2.

The size ranges are chosen to be of equal length and cover droplet diameters from zero to a diameter below which 99% of the mass of fuel falls. A total of 16 size ranges was chosen to adequately model the complete spray without using excessive amounts of computer time. The sizes range from 3.8μ to 118μ in steps of 7.6μ.

Single droplets with diameters equal to the mean of each size range are injected into the gas flow field with initial x and y coordinates corresponding to the point of sheet break-up of the spray. In addition, for each size range, droplets are injected from six different angular locations differing by 10°. Consequently the trajectories of a total of 96 fuel droplets are calculated.

The atomiser characteristics are specified by spray cone angle, velocity, distance from nozzle to sheet break-up, and the Rosin-Rammler parameters. From this and general physical data the entire spray cone is constructed.

The amount of fuel evaporated in each cell is summed for the whole spray. The mass flowrate of fuel represented by each droplet trajectory is:

$$\dot{m}_{fuel} = \frac{m_{range}}{6} \cdot \dot{m}_{total} \tag{21}$$

where m_{range} is defined in equation (20). Since each size range is represented by six droplets of different initial angular position, the factor of 1/6 occurs. The total mass flowrate of fuel is $\dot{m}_{total}$.

Results and Discussion

Droplet trajectory computations for complete sprays are presented graphically for sprays of nominal included cone angles of 45° and 80° at an injection velocity of 20m/s and also for a 45° cone angle and 50 m/s injection velocity. The injection velocity for the spray is the resultant velocity in the x-y plane acquired by each droplet as it breaks away from the liquid sheet at the point of sheet break-up. No initial tangential velocity is given to the droplets. The distance between the atomiser and the point at which this occurs has been taken as 5mm. The figures show side and end elevations of the combustor can and droplet trajectories have been projected orthographically onto these.

The large arrows indicate the air injection locations. Droplet burn-out locations are encircled, whilst trajectories ending without a circle have hit the combustor wall. In the case of the latter, calculations are terminated a short distance before the wall.

Considering figure 6 it is observed that for these typical values of cone angle and velocity (as might be expected from a pressure-jet type of atomiser), the majority of droplets are, in fact, evaporating in the two-dimensional region of the combustor can (<60μ). However, a significant proportion impinge on the combustor wall and of particular interest is the portion of the spray deflected by the primary air injection stream and hitting the opposite wall of the can. Some of the largest droplets (>100μ) are also observed to be surviving into the area near the dilution air injection having sufferred slight deflections by both primary and secondary air jets.

Figure 9 shows a histogram of the proportion of fuel evaporated along the length of the combustion chamber for the 45°, 20 m/s case. Although the relatively small proportion of fuel surviving into the three-dimensional region of the combustor can would at first appear to justify a simpler two-dimensional model of spray combustion, it must be remembered that in a field where very high combustion efficiencies are already common small losses of fuel are of increased importance. Also, in applications such as aviation, where weight becomes a major factor, small combustion inefficiencies become magnified in financial terms. In terms of pollution emissions, only a very small proportion of the fuel needs to be involved to produce significant effects.

Figures 7 and 8 show droplet trajectories for two extreme cases. Fig. 7 shows a spray with high velocity. More fuel is seen to be being deposited on the combustor wall further downstream than in the case of the 20 m/s spray. This would obviously constitute a bad choice of nozzle characteristics. In Fig. 8 the spray cone angle is clearly too large, as a significant proportion (4%) of the fuel hits the chamber wall.

Conclusions

It is shown that an analytical technique can be used to predict the details of combustion of individual droplets and the fuel spray as a whole. As a design tool such an approach would clearly be of great help to the combustion chamber designer and in the matching of nozzle characteristics.

The significance of the behaviour of large droplet sizes is demonstrated as being a likely cause of reduced combustion efficiency and the presence of pollutants in the exit gases, which may arise from locally fuel-rich areas and unburnt fuel appearing in the lower temperature regions of the combustor. An additional hazard is possible corrosion of and damage to turbine blades due to the presence of pollutants, soot and unburnt fuel droplets in the combustor exit gases.

The information obtained by means of the computer prediction is at present impossible to obtain by experimental measurements. A method has yet to be found whereby the computed results can be verified experimentally.

Acknowledgements

References

1. Swithenbank, J., Turan, A. Felton, P.G. and Spalding, D.B., "Fundamental Modelling of Mixing, Evaporation and Kinetics in Gas Turbine Combustors".

2. Boysan, F., and Swithenbank, J., "Spray Evaporation in Recirculating Flow", Seventeenth International Symposium on Combustion, Leeds, 1978. AGARD-CPP-275, Combustor Modelling, NATO, 1979.

3. Law, C.K., "Motion of a Vaporising Droplet in a Constant Cross Flow", Int. J. Multiphase Flow, 3, 299-303, 1977.

4. Chiu, H.H., Ahluwalia, R.K., Koh, B., and Croke, E.J. "Spray Group Combustion", Sixteenth Aerospace Sciences Meeting, Paper No. 78-75, Huntsville, Alabama, January, 1978.

5. Mellor, A.M., "Gas Turbine Engine Pollution", Prog. Energy Combust. Sci., 1, 111-135, 1976.

6. Dring, R.P. and Suo, M., "Particle Trajectories in Swirling Flows", Journal of Energy, Vol. 2, July-August, 1978, pp. 232-237.

7. Dring, R.P., Caspar, J.R. and Suo, M., "Particle Trajectories in Turbine Cascades", Journal of Energy, Vol. 3, May-June, 1979, pp. 161-166.

8. Dickerson, R.A. and Schuman, M.D. "Rate of Aerodynamic Atomization of Droplets", Journal of Spacecraft & Rockets, Vol.2,99, 1965.

9. Wise H., and Agoston, G.A., "Literature on the Combustion of Petroleum". American Chemical Society, Washington, D.C., 1958.

10. Frossling, N., Gerlands Beitr. Geophys., 52, 170 (1938).

11. Ranz, W.E. and Marshall, W.R., Chem. Eng. Prog. 48, 141, 173 (1952).

12. Turan, A., "A Three-Dimensional Model for Gas Turbine Combustors". Univ. of Sheffield, Ph.D. Thesis. September, 1978.

13. Pan, Z., Private Communication.

List of Figures

Fig. 1

Fig. 1. Geometry of Lycoming combustor can
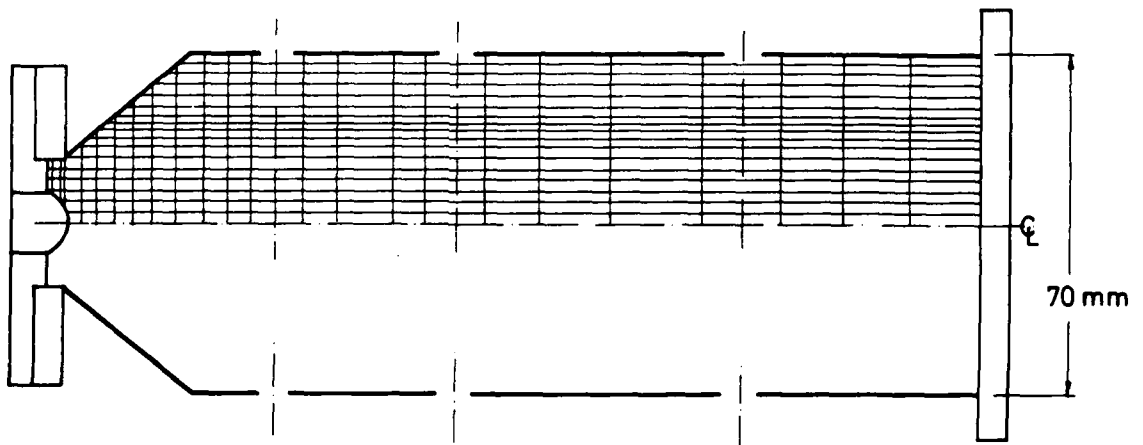
LYCOMING COMBUSTOR,
GRID ARRANGEMENT   27 x 18 x 7   =   3 402 TOTAL POINTS

Fig. 2

Fig. 2. Finite difference grid for the Lycoming combustor can
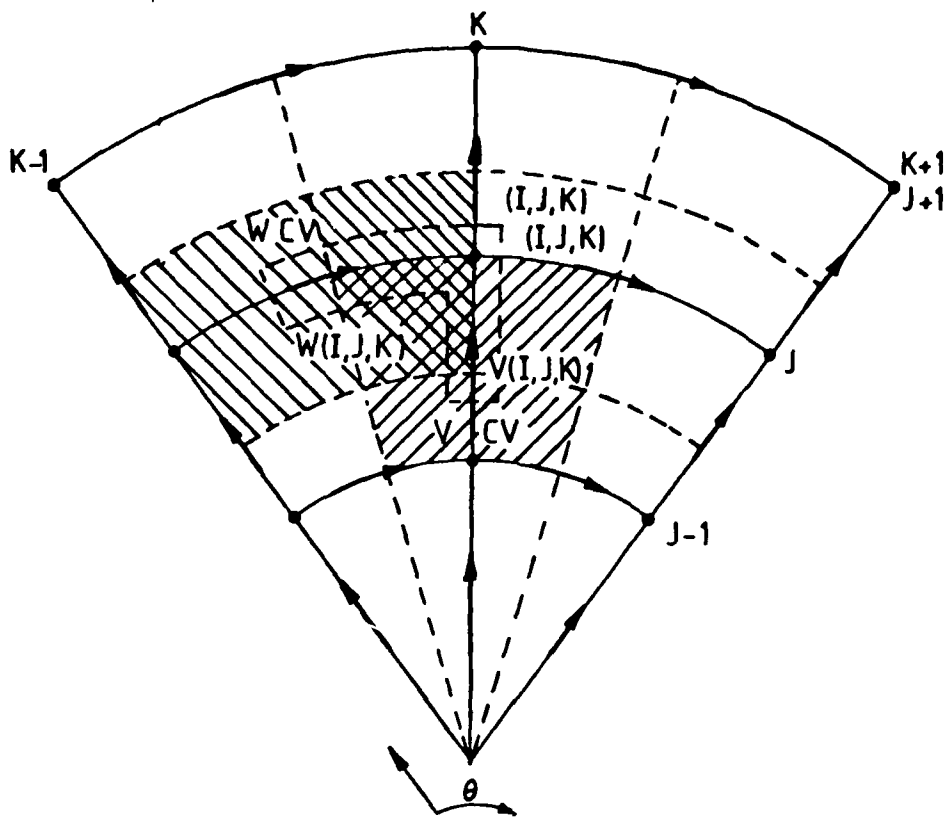
W- AND V-VELOCITY CONTROL VOLUMES IN -θ DIRECTIONS.
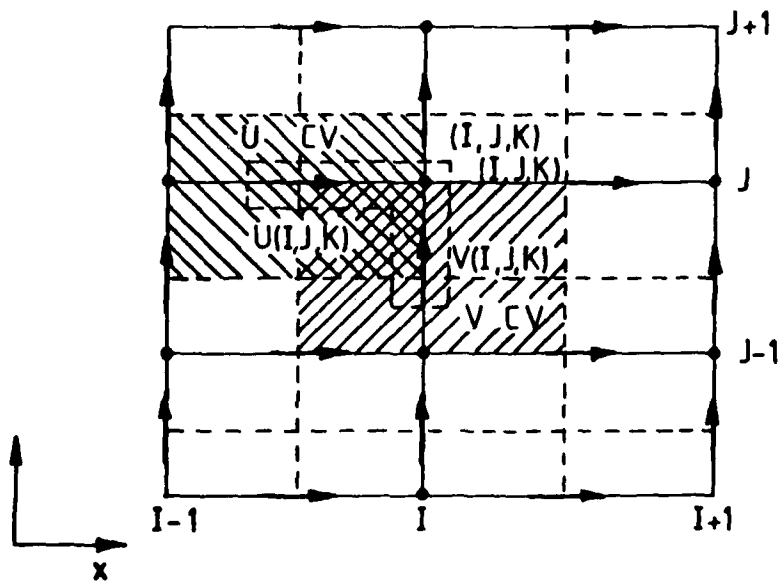
U- AND V-VELOCITY CONTROL VOLUMES IN -x DIRECTIONS.

Fig. 3. Location of u-, v- and w-velocity control volumes

Fig 3

Fig 4
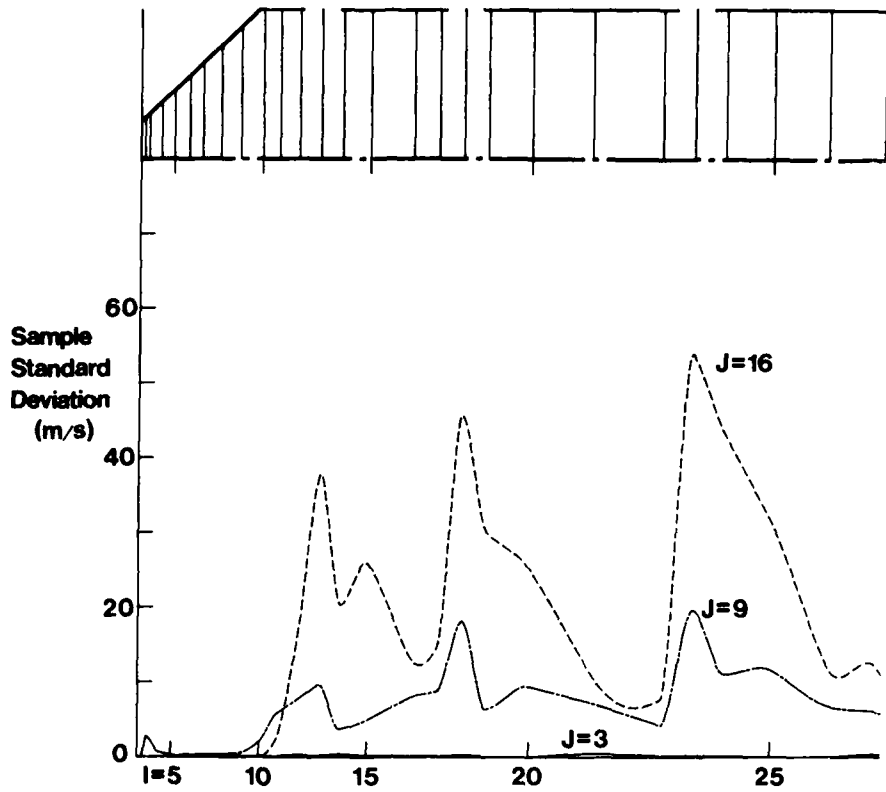
Fig. 4. Angular Variation of U-Velocity

K = 4

I = 13
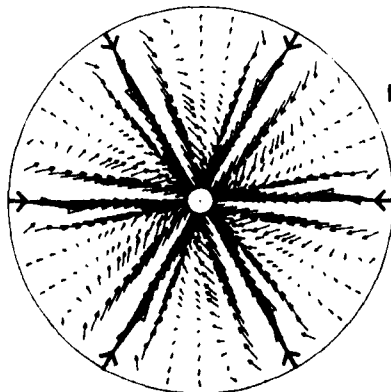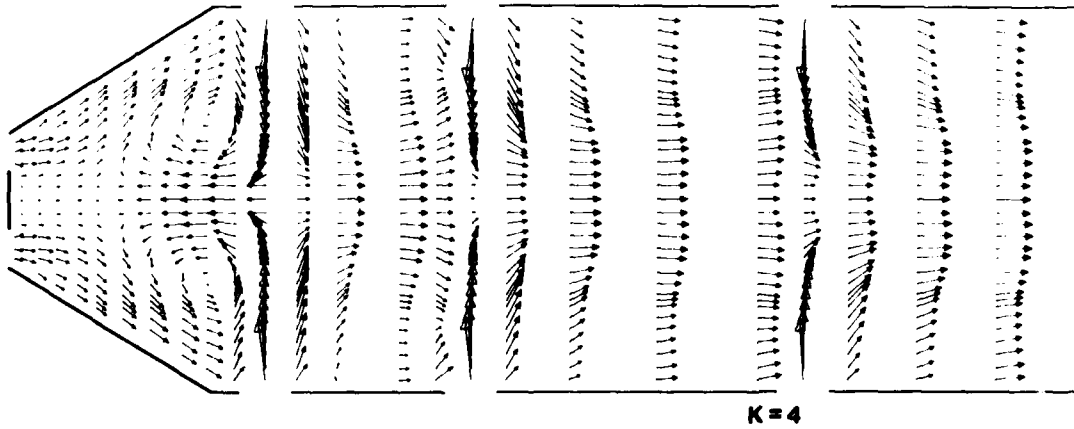
SCALE

→

100 m/s

Fig. 5

Predicted Velocity Field for Lycoming Combustor

at Air Injection Planes
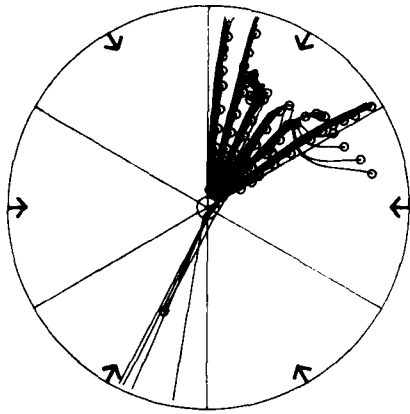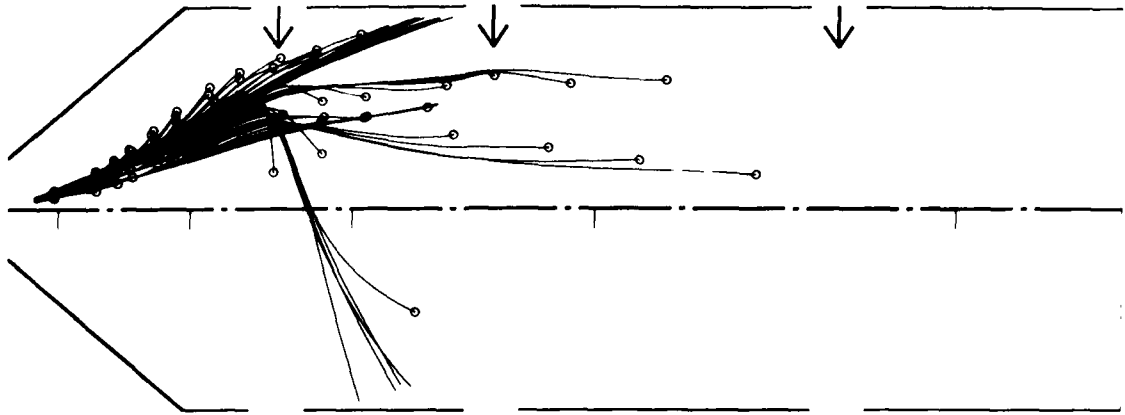
Included cone angle : 45°

Injection Velocity : 20 m/s

Fig.6 Droplet Trajectories for Complete Spray
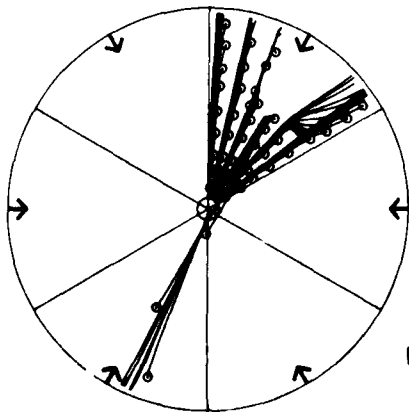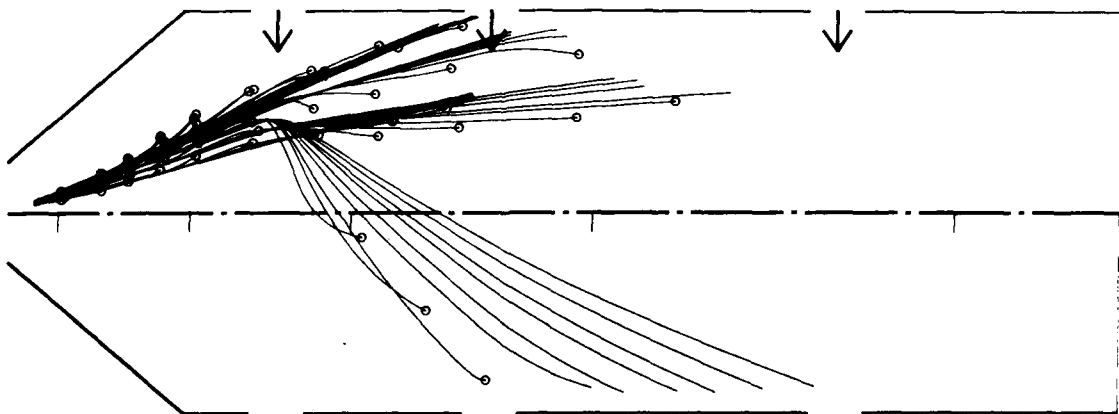
Included cone angle : 45°

Injection velocity: 50 m/s

Fig.7 Droplet Trajectories for Complete Spray
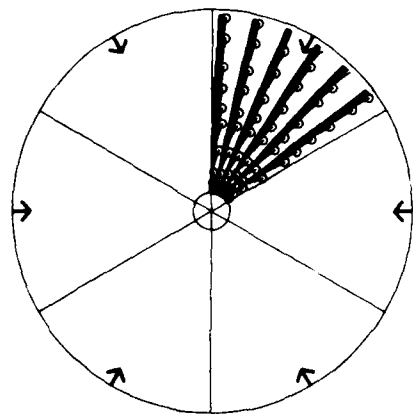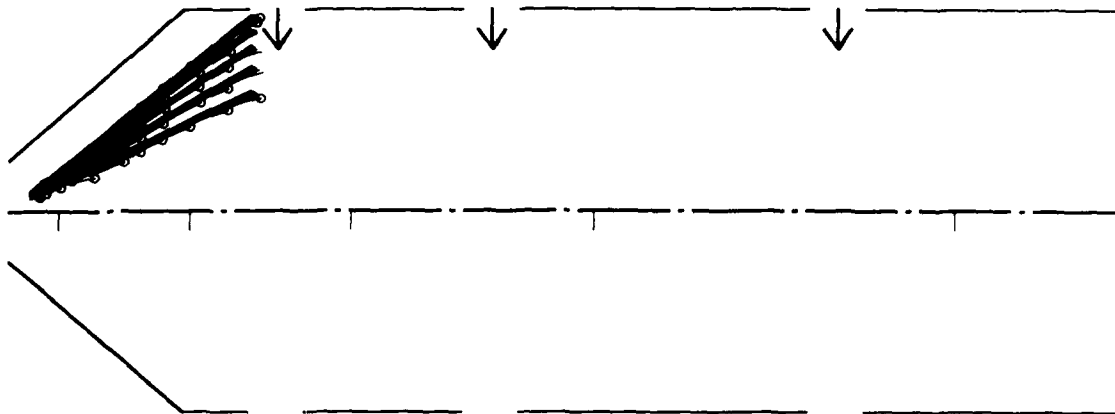
Included cone angle : 80°

Injection velocity : 20 m/s

Fig.8 Droplet Trajectories for Complete Spray

$$\frac{\Delta \dot{m}}{\Delta x}$$

Area
= $\dot{m}_{TOTAL}$

I=5   10   15   20   25
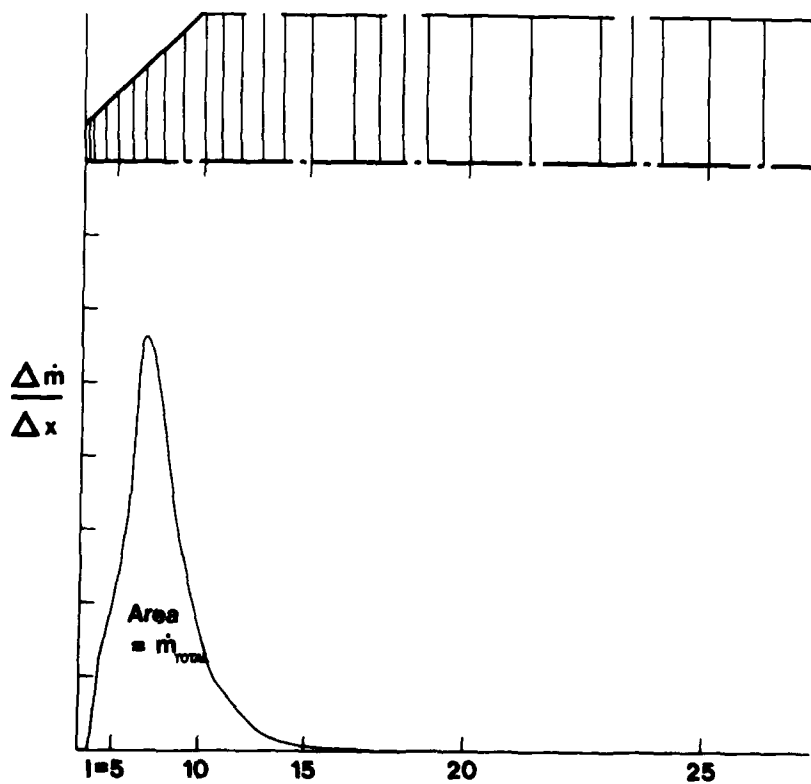
Fig 9

Fig. 9. Histogram of mass flowrate of fuel vapour vs. x-axis